JPRS-UEQ-91-011
29 OCTOBER 1991

JPRS Report

Science & Technology

USSR: Engineering & Equipment

Science & Technology
USSR: Engineering & Equipment

JPRS-UEQ-91-011 29 October 1991

CONTENTS

Analyzing the Load-Bearing Capacity of Fiber Composite Structures

917F0335B Kazan IZVESTIYA VYSSHIKH UCHEBNYKH ZAVEDENIY: AVIATSIONNAYA TEKHNIKA in Russian No 1, 1991 pp 76-80

[Abstract of article by V. A. Zarubin]

UDC 539.4

[Abstract] A method of analyzing the load-bearing capacity of a fiber composite structure was presented. The model used in the analysis was a finite-element, aerodynamic model of a forward-swept wing with a D-16 aluminum-alloy frame and graphite-fiber composite skin with a 0°(90°)+45° lay-up of unidirectional layers. (Data on physical and mechanical properties were provided). The analysis takes into account the physical and geometric non-linearity and the aeroelastic non-linear effects associated with the redistribution of aerodynamic load during non-linear deformation of the structure, i.e., failure of the binder and crack origination, change in structural shape, and change in aerodynamic load during non-linear deformation. Physical non-linearity is solved by calculating the stresses for each iteration in each layer of each element according to some strength criterion predicting binder failure, and the layers in which the binder will fail are identified. Geometric and aeroelastic non-linearity are determined iteratively by adding at every step of the process the displacements from the preceding iteration to the coordinate loci of the model. The system of non-linear equations, the solution algorithm, and the theoretical load conditions necessary to analyze the load-bearing capacity of the wing model were provided. Figures 3; references 8: 7 Russian, 1 Western.

Designing a Language Processor for Aircraft Engine Testing

917F0335A Kazan IZVESTIYA VYSSHIKH UCHEBNYKH ZAVEDENIY: AVIATSIONNAYA TEKHNIKA in Russian No 1, 1991 pp 65-68

[Abstract of article by Yu. V. Kozhevnikov and I. A. Zalyayev]

UDC 629.7.03.001.4-52

[Abstract] The problems involved in designing a language processor for aircraft engine testing systems were described, and a methodology for designed such a language processor was presented. When designing a language processor, three main concepts should prevail: 1) the software should contain a "Design Engineer" component that engages in a dialog with the user when the calibration parameter values for the required testing procedure are set; each software module that conveys the parametrically calibrated testing operations within the system should be translated from the basic standard programming languages into the loading language of the operating system of the automated aircraft engine testing system; all the loading software modules should be combined into a single software package that can implement the required testing technology; 2) the software should contain a "Consultant" component that informs the user of the post-testing output data, of the validity of the output data, of deviations in the output data and their causes, and of recommended courses of action; 3) the user should be able to consult the system for information about specific testing technologies. There are also three main principles that should be adhered to during language processor design: 1) matrix decomposition, which breaks down a complex language processor design problem into relatively simple interrelated elements; 2) standardization of the component elements of the processor in order to ensure that standard procedures are followed when they are modelled, designed, and used; 3) parametric calibration capability for standardized elements for specific applications. As an example of how this methodology can be applied, it was used to design a language processor for the mathematical processing of testing system measurement data. The processor, which requires no more than 25K of memory, was written in FORTRAN-77 and run on an SM-4 computer. Figures 2; references 2: Russian.

Optical System for Shaping Laser Beams Into Shiftable Stricture of Same Width at Various Distances From Laser Cavity

917F0355A Moscow IZVESTIYA VYSSHIKH UCHEBNYKH ZAVEDENIY: GEODEZIYA I AEROFOTOSYEMKA in Russian No 6, Nov-Dec 90 pp 90-95

[Article by Y.M. Klimkov, doctor of technical sciences, professor, Moscow Institute of Geodetic, Aerial Photography, and Cartographic Engineers]

UDC 535

[Abstract] An optical system consisting of two components with a short- focus first component behind the exit mirror of a confocal laser cavity is considered for shaping a reference laser beam into a stricture shiftable without change of width to various target locations along the path, measurements made with such a laser beam being not only more accurate but also more uniformly accurate than those made with a collimated one. With such a beam, moreover, the range of measurements can be extended to farther distant targets and the detrimental effect of laser radiation on all targets is eliminated as long as the radiation power within the stricture remains lower than maximum allowable. Either one of the two components is movable along the optical axis of the system and the focal length of either one can varied. The problem of ensuring a constant width of a shiftable stricture cannot be solved by only moving the components or by only varying their focal lengths, however, as is demonstrated on a Gaussian laser beam leaving a confocal laser cavity while carrying radiation of a given wavelength. Following an analysis of the problem based on applicable relations of geometrical laser optics, two such systems are designed in accordance with this principle for a single-mode TEM_{00} laser beam: one with a variable focal length of the second component and one with a variable focal length of the first component. In the first case are given the radiation wavelength, the confocality index of the laser cavity, both width of the neck and location of its plane along the optical axis, also the allowable variation of its location. In the second case the focal length of the second component is assumed to be minimal and constant. In both cases are calculated the distance through which the respective component needs to be moved. Figures 2; references 1.

Laser Interference-Type Alignment Protractor With Stabilized Beam

917F9355B Moscow IZVESTIYA VYSSHIKH UCHEBNYKH ZAVEDENIY: GEODEZIYA I AEROFOTOSYEMKA in Russian No 6, Nov-Dec 90 pp 96-100

[Article by V.M. Ukrainko, candidate of technical sciences, docent, Novosibirsk Institute of Geodetic, Aerial Photography, and Cartographic Engineers]

UDC 528.5

Abstract] A method of stabilizing the position of a laser beam by immunization against instability of its radiation pattern is proposed, for application in various optical instruments. It is based on the law of reflection and its corollary that a change of the incidence angle will result in an equal change of the reflection angle, in the opposite sense upon a single reflection or any odd number of reflections and in the same sense upon two or any other even number of reflections. Splitting the laser beam into two equal ones with half the total energy in each and reflecting one of them an odd number of times while reflecting the other an even number of times will make it possible to use both as a geodetic reference line and to immunize geodetic measurements against any drift of the laser beam in space, including the parallel shift of the reflected beam attending a change of the reflection angle. Compensation of the instability of the laser radiation pattern, specifically of the orientation of its axis, is based on the mathematical relation $r - s = 2t + 1$ (r- number of reflections of one beam, s- number of reflections of other beam, t= 1,2,... series of natural numbers). When the difference between the number of reflections of one beam and the number of reflections of the other beam is an odd number, then the two beams deviate in opposite senses in a compensatory manner. This principle has been applied to an instrument for measuring misalignments by the interference method. The instrument consists of a setting device and a pickup device. The setting device includes a laser, a collimator, a zonal plate, and two prisms: a pentaprism and a right triangular prism joined together along their faces with right corner angles. The vertical axis of this prismatic optical system passes through the diagonal face of the triangular prism and the center of the pentaprism so that it coincides with the axis of a mechanism by means of which the setting device is centered above a reference point. When the laser beam entering the prismatic optics is stable, then the two half beams leaving the prisms coincide. When the entering laser beam is unstable, then the half beams leaving the prisms are misaligned but so that their center of energy does not shift and measurements relative to this center can proceed. The pickup device includes a photodetector for sensing the laser beam, milliammeter, a clock-type indicator with 0.01 mm scale divisions acting as sensor of linear displacements, and a micrometer screw. The photodetector is split along the line which coincides with the axis of pickup centering mechanism and its position is adjusted by means of a micrometer screw till it senses the center of laser energy on the basis of the milliammeter readings. As source of coherent light can serve the LGN-105 gas laser of a commercial laser range finder and as collimator can serve the sighting tube of an OT-02 theodolite. The mean-square error of misalignment measurement m_Q^2 is essentially the sum of three components: mean-square error of the linear-displacement sensor m_s^2 + mean-square error of pickup centering m_c^2 + mean-square error of setting reduction m_r^2. On this premise, under laboratory conditions this instrument can measure up to

10 mm large misalignments over a 30 m long distance accurately within 0.05 mm. Figures 4; references 5.

Determining the Composition of Surface Optic Layers Made With Rare-Earth and Zirconium Oxides

917F0326A Moscow ZAVODSKAYA LABORATORIYA in Russian No 3, 1991 pp 12-14

[Abstract of article by V. T. Mishchenko, L. P. Shilova, and T. M. Shkolnikova; Physical Chemistry Institute imeni A. V. Bogatskiy of the Ukrainian Academy of Sciences, Odessa]

UDC 546.831:546.65:543.24

[Abstract] The objective of this study was to develop a simple method of determining the composition of optic oxide layers thermally sprayed onto glass or quartz substrates. It was also hoped that this method could be used to detect any difference between the composition of these layers and that of the tablets used for the coating stock. The substrates used in the tests had a working surface area of about 7 sq cm. The coatings were from 0.1 to 0.4 μm thick and were applied by electron-beam vapor deposition. The coated substrates were carefully cleaned, weighed on a scale, and placed coated side down in a beaker into which 2.5 to 3.0 ml of concentrated sulfuric acid was poured, with 1 g of ammonium sulphate added to raise the salt concentration. The contents were shaken and then boiled for 30 to 40 minutes, after which the substrate was removed and the excess sulfuric acid boiled off. The solution was transferred to a 25-ml column and diluted with distilled water. The substrate was cleaned and reweighed. The zirconium content was determined by titrating this solution and using a formula to calculate the weight % of the zirconium oxide. Rare-earth oxides were determined analogously, using the solution that had been titrated to determine zirconium oxide content. The results of oxide content determined by titration were nearly identical with the results of oxide content determined gravimetrically. A variation of this method was used to find that the composition of the coatings and the tablets was identical. Tables 1; references 8: Russian.

Geomagnetic Survey of Ocean Bed From Towboat

917F0289A Moscow OKEANOLOGIYA in Russian Vol 31 No 2, Mar-Apr 91 pp 332-341

[Article by V.S. Yastrebov, G.M. Valyashko, A.M. Gorodnitskiy, and N.A. Rimskiy-Korsakov, Institute of Oceanography imeni P.P. Shirshov, USSR Academy of Sciences, Moscow]

[Abstract] A technique and the necessary apparatus for geomagnetic survey of the ocean floor in search of useful ore deposits underneath have been developed at the Institute of Oceanography and the Geomagnetic Research Laboratory, such a survey including simultaneous measurement of the floor depth with a towed Zvuk("Sound")-6 probe. The apparatus consists of an echo sounder, a portside and starboard lateral-scan sonar set, an acoustic profilograph, and MPM-6 proton magnetometer, a stereoplanigraph, and a television system. The sonar and the acoustic profilograph produce images of the floor surface, these images being recorded by a set of INEY-P facsimile receivers and then photographed. The proton magnetometer reads the magnitudes of the resultant geomagnetic field vector which, after conversion form analog to digital form, are displayed graphically by a KSPP recording instrument. The magnetometer operates in 4 s long cycles and the nacelle carrying it is towed with a special cable 18 m behind the probe. The depth of the probe under the water surface is monitored by the echo sounder and controlled by an anchor windlass, a feature not needed and not included in hydromagnetic surveys of the ocean surface. The entire Zvuk-6 surveying and measuring apparatus was tested in the northeastern part of the Atlantic Ocean, over a 2 km square area of a plateau above the northeastern slope of the Cruiser seamount where the depth of its surface changes from 1500 m to 1800 m. The geomagnetic survey data were processed in two stages according to a specially devised procedure, in the first stage readings taken at the various altitudes above the ocean floor being all reduced to one altitude above the ocean floor in a plane conformal with the bed relief or to one depth in a plane parallel to the ocean surface. In the second stage was calculated the discrete Fourier cosine transform of the geomagnetic potential field, already referred to a given surface, and mathematical problems pertaining to interpretation of the data were solved for a subsequent quantitative analysis. One such problem was evaluating the effective magnetization of a magnetically active bedrock layer on the basis of magnetometer readings, with the geometry of that layer known from the survey. Inasmuch as the magnetometer readings included a random interference, it was necessary to estimate this interference with the aid of a correlational discriminator before corrections were made for the depth variation of the of the ocean floor. The thus evidently ill-conditioned Fourier transformation problem was solved by the method of adaptive regularization applicable to linear ill-conditioned problems in geophysics and useful for processing spectra of compound signals. The optimum regularization parameter was determined on the basis of the orthogonality principle. According to the thus analyzed and interpreted results of this experimental geomagnetic survey, the ocean bed under the eastern slope of the Cruiser seamount is about 80 million years old. Its normal magnetic field, calculated with the aid of IGRF-85 coefficients, has a minimum intensity of up to 6 mOe at 30-60 m above the ocean floor and a maximum intensity of up to 450 mOe at 80 m above the ocean floor. Figures 5; references 23.

Making Silver Halide Materials More Versatile by Improving Image Development Techniques

917F0326B Moscow ZAVODSKAYA LABORATORIYA in Russian No 3, 1991 pp 25-26

[Abstract of article by G. M. Korzun, A. V. Brublevskiy, and S. K. Rakhmanov; Scientific Research Institute of Physical Chemistry Problems at Belorussian State University imeni Lenin, Minsk]

UDC 778.33

[Abstract] This article describes two ways to improve the quality of x-ray image development. The first method is known as the silver dispersion method, or MDS, and is based on decreasing the size of the silver particles that form the image. This method is used after the film has been exposed using standard methods in either natural or artificial light. It entails bleaching the silver image in a solution based on potassium hexacyanoferrate and alkali metal halide at 20+/-2°C for 1 to 3 minutes, rinsing it in running water for 1 to 2 minutes, and then enhancing the image in an alkaline solution made with a strong reducing agent (e.g. tin dichloride). The addition of silver ion ligands is optional. The other method utilizes the emulsion microcrystals that usually do not help to form the visible image during standard x-ray film development. This is done by modifying the process: the film is developed for 2 minutes at 20°C in a developer to which silver ion ligands have been added. It is then rinsed in running water for 1 minute, fixed in BKF-2 fixer for 4 to 6 minutes, and rinsed in running water for 10 to 15 minutes. The MDS method can be used with any type of silver halide x-ray material, reduces irradiation time 2.5 to 4-fold without compromising radiographic sensitivity, improves image contrast, enhances previously developed images of poor quality, and makes it possible to use a wider range of radiographic materials and equipment. The second method reduces irradiation time 2 to 4-fold while increasing radiographic sensitivity, and makes radiographic testing processes more productive and cost-efficient. Tables 1; references 9: 7 Russian, 2 Western.

Analyzing Disperse Composition of Corrosion Products in Dukovany Nuclear Power Plant Coolant Circuit and RVS-3 Reactor Loop

917F0344A Moscow TEPLOENERGETIKA in Russian No 5, May 91 pp 74-77

[Article by M. Zmitko, S.A. Tevlin, Moscow Power Engineering Institute]

UDC 621.311.25:621.039.628.147.22

[Abstract] Corrosion product (PK) samples taken from the third generating unit of the Dukovany nuclear power plant (AES) and the RVS-3 reactor water loop at the Nuclear Research Institute of the Czech and Slovak Federal Republic are investigated in order to determine their degree of dispersion, chemical composition, and morphology. Coolant samples from the primary circuit of the Dukoviny AES were taken using standard sampling lines whereby corrosion products were retained by microfilters with a 25 mm diameter and 0.4 μm pores. Coolant samples from the RVS-3 reactor loop which simulates the principal thermal and hydraulic parameters and water chemistry conditions of water-cooled water-moderated power reactors (VVER) were taken using a sampling system which first cools the samples to 40°C and then passes them through the same microfilters. Sampling characteristics and some coolant characteristics are summarized. The samples were subjected to a gamma spectroscopy analysis to determine the radionuclide composition and elemental analysis by means of atomic adsorption spectrometry (AAS). The dispersion degree spectrum of the corrosion product particles trapped by the filters and their shape were determined by a scanning electron microscope (SEM). The elemental composition of individual corrosion product particle types was determined by an energy analysis of scattered X-rays by an EDAX system. As a result, the specific radioactivity of the Cr-51, Co-58, Mn-54, Fe-59, and Co-60 nuclides and percentage concentration of Fe, Cr, Ni, Mn, Co, Mg, and Al were determined. It is shown that the Cr-51 nuclide is the most active while particles consist primarily of Fe (40-100%). The experiment confirmed known data on the particle dispersion spectra and made it possible to obtain additional information about the discrepancy of the particle composition and steel composition. References 12: 2 Russian; 10 Western; figures 5; tables 4.

Asynchronous Maglev Transport Vehicle

917F0314A Novocherkassk IZVESTIYA VYSSHIKH UCHEBNYKH ZAVEDENIY: ELEKTROMEKHANIKA in Russian No 1, 1991 (manuscript received Jun 90) (after revision 15 Dec 90) pp 36-42

[Article by I. I. Talya, V. I. Serebryakov, A. P. Yepifanov, et al.]

UDC 621.313.333012:[621.439:621.318]

[Text] The design of electromechanical devices, intended for development of thrust force and the force of electromagnetic suspension of a transport vehicle, is described. The results of experimental study of the magnetic field in the gap, and of the thrust and normal forces in the static mode are presented. It is shown that there is no electromagnetic coupling of the excitation winding and armature winding in the developed device. The armature winding does not effect the normal force created by the magnetization winding in the operating mode. The proposed design supports energy indicators of 1.3-1.5-fold higher than in individual systems in asynchronous thrust and suspension with modular configuration.

The tendency to use two-function electromagnetic devices for the linear electric drive and magnetic suspension system has been noted in recent years in development of high-speed passenger transport vehicles [1-3]. Compared to separate thrust and magnetic suspension systems [4, 5], they permit a reduction of the mass and overall dimensions, the use of more effective configuration circuits for the drive and suspension, an increase of payload, an increase of the energy indicators of the drive, a reduction of the requirements on the accuracy of laying the roadbed, and consequently, a reduction of its cost.

Combination drive and magentic suspension systems are ordinarily worked out on the basis of a linear synchronous electric motor, when a three-phase armature winding is located either in the track [1] or together with the excitation winding on a moving inductor [2, 3] (inductor type of motor). These systems have a number of disadvantages along with the above advantages:

1. The excitation winding of the motor is used simultaneously to create suspension of the carriage and, consequently the magnetic flux must be kept essentially constant, while the thrust force can be regulated only from the direction of the armature winding: by the value of current and by the load angle θ. In reality, due to restriction of the effect of the reaction of the armature to the suspension force, angle $\theta \leqq 25°$, and regulation can be accomplished by the current of the armature winding. The multiplicity factor of the starting current $K_I = I_s/I_l$ in start modes should be equal to the multiplicity factor of the start force $K_F = F_{xs}/F_{xl}$. The largest cross-section of the armature winding must be laid in this regard when developing these systems to guarantee thermal overloads in starting modes.

2. The track armature winding LSD and the ferromagnetic modules LID are made with a specific band division τ, which eliminates their universality for urban ($v \leqq$ 70 km/hr), suburban ($v \leqq 250$ km/hr) and long-distance ($v \leqq 400$ km/hr) transport and the possibility of varying the strip separation when improving the drive on the basis of the operating experience of these systems.

A new asynchronous maglev module (HELM) [6], developed for the drive and electromagnetic suspension of a carriage weighing 40 t of an experimental transport system, is free of the indicated deficiencies. An experimental model was manufactured for stand tests. The layout and overall view of this module are presented in Figure 1.

The ATLM has been realized successfully in a modular drive system, the main design principles of which and the positive aspects have been described in detail in [7, 8]. The arrangement of the ATLM inductors on the sides of the carriage in the form of a continuous chain with minimal possible motion of the gaps L_p between them and corresponding shifts of the NS [not further identified] of the armature windings of adjacent inductors [8]. The inductors can be arranged in groups, the distance

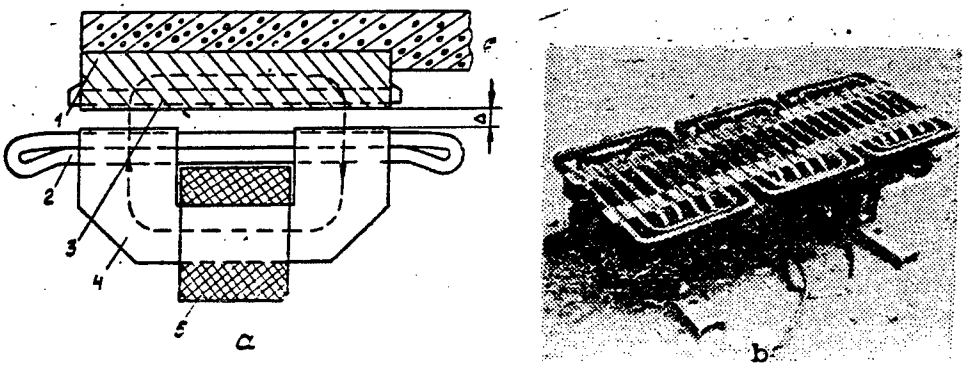

Figure 1. Diagram (a) and General View (b) of ATLM Inductor

between which should be adequate to damp the eddy currents behind the trailing edge of the latter in the module group with the carriage version of the travel part.

The ATLM inductor contains a U-shaped core 4, the pole projections of which are assembled of sheet steel. A magnetization winding 5, designed to create a suspension force and fed from a DC source through an automatic regulator (short-circuiting path of the magnetic flux of winding 5 is shown by the dashed line), is located on the inductor armature. A short-circuited winding 3 of the "squirrel cage" type is located in the grooves of the reverse magnetic surface (OM) 1, which can be laminated or in one piece. The three-phase armature winding 2 is located in the grooves of the pole projections of the inductor core. With symmetrical arrangement of the inductor with respect to the track structure, the emf induced in the rod elements above different pole projections are equal in value and counterdirected; therefore, the possibility of creating a braking force is eliminated. There are seemingly two inductors with longitudinal short-circuiting of the magnetic flux with the general winding, operating to one track structure, with respect to the tractive force. We note especially that a variable magnetic flux $\Phi_{\sim}$ is superimposed in the air gap to the constant Φ^{-} and, accordingly, the linear load for variable current is limited by the conditions of saturation of the teeth of both the inductor and of the magnetic circuit at given value of suspension force. This is a common disadvantage of these combination systems, including those based on an inductor motor. The design of the ATLM also eliminates the mutual induction coupling of the magnetization winding with the armature winding, since the axes of these windings are mutually perpendicular.

Tests of the manufactured module were conducted in static modes with the magnetization winding fed by direct current and with the armature winding fed by alternating current at frequencies close to absolute slips $f_2 = s \times f_1$, and were kept constant with different distribution of currents by phases, corresponding to the instantaneous values of alternating current. The studies included a check of the inductive coupling between windings, determination of the dependence of induction of tractive and normal forces in the gap on the ratio of the magnetizing forces of the magnetization winding and armature winding. The emf induced in the armature winding does not exceed 4% of the phase voltage when the magnetization winding is fed by industrial frequency current equal in value to the rated current, which confirmed the initially suggested absence of inductive coupling between windings.

The induction distribution curves in the gap along the inductor at rated magnetization current and with DC power of the armature winding, corresponding to a moment of time when $i_{a1} = I_m$, are presented in Figure 2. It is obvious that the constant components of induction on the surface of both pole projections are equal in value and are oppositely directly. Accordingly, creation of a braking force in the suspension system is eliminated with

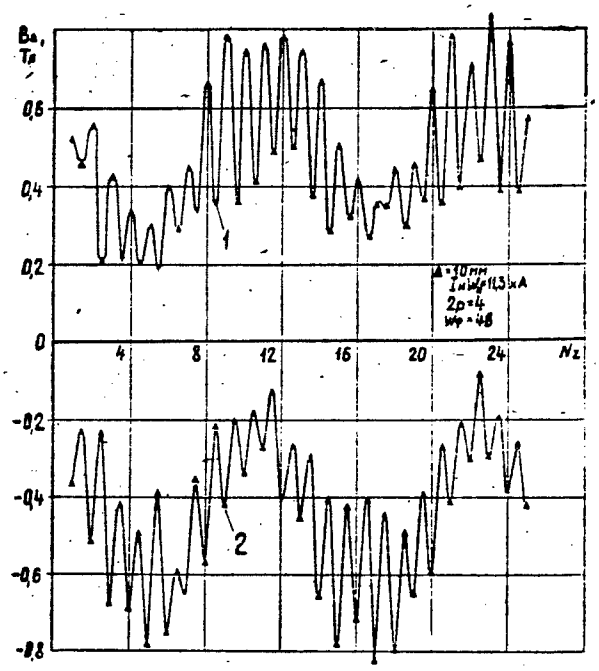

Figure 2. Distribution of Normal Magnetic Induction Component on Surface of Strip Projections Along Length of ATLM Conductor Between Inductor and Track Element of 10 mm and of NS of Magnetization Winding $I_m W_m$ = 11.3 kA: 1—left pole projection; 2—right pole projection

a short-circuited track structure. The variable components of the magnetic component in the gap, created by a three-phase anchor winding, are aligned accordingly and create a tractive force. The scattering flux between the pole projections of the magnetization winding is increased somewhat and as a result the constant component of the magnetic field in the gap is reduced as the linear current load increases. Quantitatively, this reduction is dependent on the ratio of the magnetizing forces of the windings (Figure 3), it is dependent on slip in operating modes. Thus, the decrease of the constant component of the field in the gap does not exceed 4% in the operating mode at nominal values of currents in both windings.

The foregoing has a direct influence on the dependence of the suspension force on the variable component of the field in the gap. This problem was studied especially in the static mode with different schemes of feeding the armature winding with direct and alternating current (Figure 4). The effect of the armature winding on the normal force, created by ther suspension system, has not been established upon variation of the linear current load to 380 A/cm (A_1 = 300 A/cm) and frequencies of f = (5-10) Hz, and, accordingly, the final result is determined by the value $B_{\Delta y} \approx$—the resulting variable magnetic field—rather than by the value of the linear load A_1.

The experimental dependence of the thrust force of the ATLM on the frequency and linear current load of the

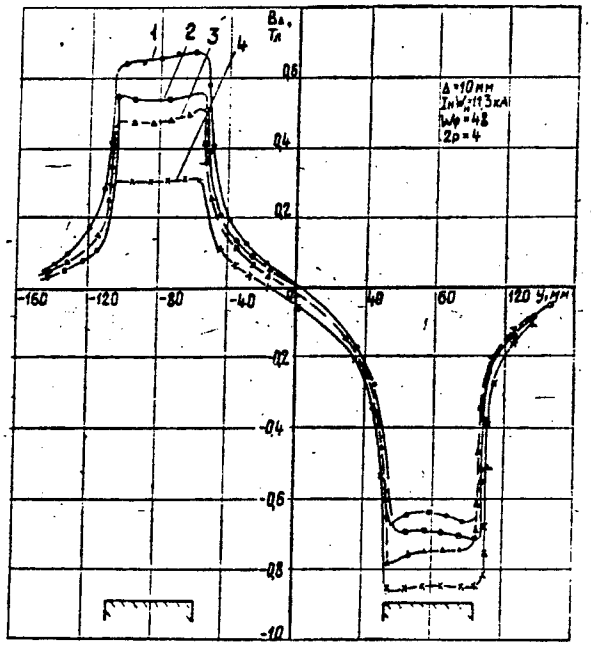

Figure 3. Distribution of Normal Component of Magnetic Induction by Width of 17-Tooth ATLM Inductor With Mechanical Gap Between Inductor and Track Element of 10 mm and NS of Magnetization Winding of I_mW_m = 11.3 kA: 1—$i_{a1} = i_{a2} = i_{a3} = 0$; 2—$i_{a1}$ = 42 A, i_{a2} = -24.5 A, i_{a3} = -18.5 A; 3—i_{a1} = 66 A, i_{a2} = -37 A, i_{a3} = -29 A; 4—i_{a1} = 120 A, i_{a2} = -67 A, i_{a3} = -53 A

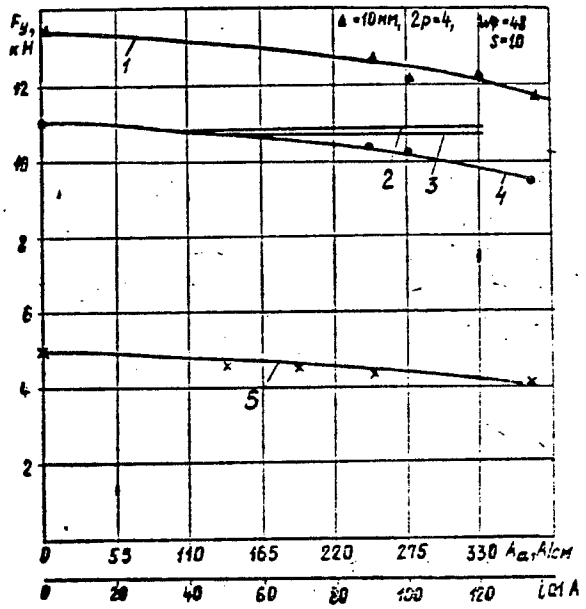

Figure 4. Experimental Functions of Normal Force in Static Mode on NS of Magnetization Winding I_mW_m, Frequency f_1 and Linear Current Load of Armature Winding (Curves 2, 3), on Current Amplitude of Armature Winding When It Is Fed by Direct Current ($i_{a1} = I_{ma}$, $i_{a2} = i_{a3} = -0.50I_{ma}$, Curves 1, 4, 5)

armature winding when it is fed from a static frequency converter (SPCh) is presented in Figure 5. These results can be considered as the characteristics of the tractive force due to the slip frequency in case of weak manifestation of the end effect, for example, with modular configuration of the drive with a large number of these ATLM. It is also obvious that the linearity of the magnetic circuit is maintained at 1.5-multiple overload with respect to current, i.e., $F_x \equiv i_a$. Accordingly, the required starting forces can easily be achieved. Thus, for example, the rated tractive force of 10 kN is realized at f_2 = 13.5 Hz and A_a = 289 A/cm for a suburban passenger car (v ≦ 250 km/hr) weighing 40 t, on each side of which 18 inductors are located. The required starting force of 33 kN per car is achieved at f_2 = 8 Hz and A_a = 415 A/cm, i.e., with 1.5-multiple load for the current of the armature winding compared to the rated value.

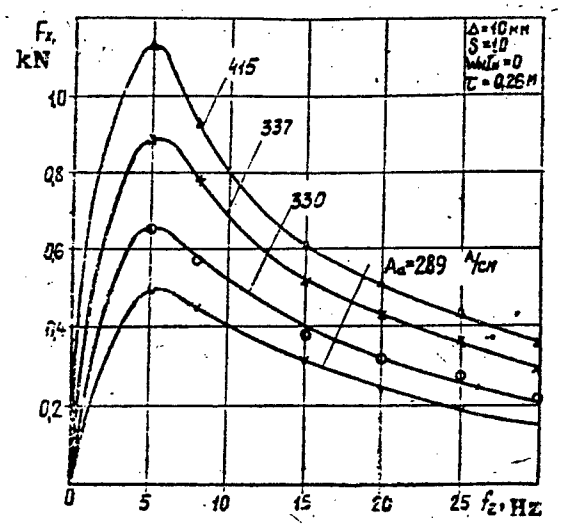

Figure 5. Experimental Dependence of Tractive Force of ATLM in Static Mode on Slip Frequency and Linear Current Load of Armature Winding With Aluminum Short-Circuiting Winding

The calculations of the operating characteristics of one side of a drive of 18 four-pole modules, according to the method outlined in [8] for a carriage of the developed experimental operating transport system, showed (Figure 6) that the results of the calculation and experiment are in good agreement by the tractive force and absolute slip f_2.

It should be noted in conclusion that an electromagnetic suspension and linear electric drive system based on the ATLM has good configuration properties and mass and size indicators, provides an energy factor of $\eta \times \cos\varphi$ at the level of 0.45-0.50, which is considerably higher than that of the commercial carriage in Birmingham [5] and of the experimental HSST-03 car. Besides transport with

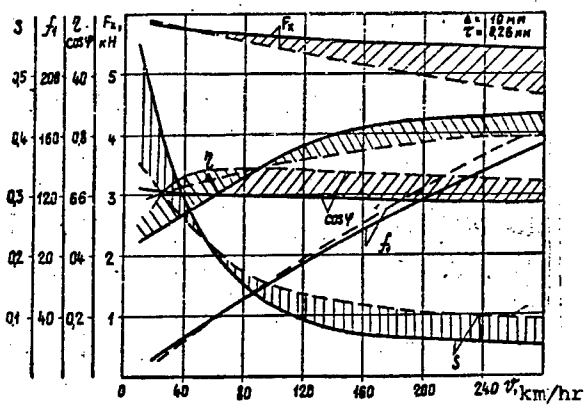

Figure 6. Calculated Dependence of Traction Parameters of Asynchronous TLM on Speed at 2p = 4 x 18, at Linear Current Load of A_a = 300 A/cm and at Slip Values of $S_m(F_x = F_{xm})$ and S_e(x cos - max)

an electromagnetic suspension, the ATLM can be used efficiently to drive a high-speed trolley with electromagnetic relief of the wheel and can be used in industrial suspension units with linear electric drive.

Bibliography

1. Raschbichler, H. G., Wacker, M. Status of the Maglev and Linear Drive Technology Program in the Federal Republic of Germany, International Conference on Magnev and Linear Drives, Las Vega, May 19-21, 1987.

2. Boldea, I., Trica, A., Popusoiu, G., Nasar, S. A. Field Tests on a Maglev With Passive Guideway Linear Inductor Motor Transportation System, IEEE TRANSACTIONS ON VEHICULAR TECHNOLOGIES, Vol 37, No 4, 1988.

3. Talya, I. I., Serebryakov, V. I., Suslova, K. N. et al. "Linear Electric Drive and Magnetic Suspension System Based on Linear Inductor Electric Motor for Urban and Suburban Transport Car," "Elektrovozostroyeniye: Sbornik nauchnykh statey" [Electric Locomotive Construction: Collection of Scientific Articles], Vol 31, Novocherkassk, Novocherkasskiy politekhnicheskiy institut, 1990.

4. Nenadovic, V., Riches, E. E. Maglev at Birmingham Airport, GEC REVIEW, Vol 1, No 1, 1985.

5. Suzuki, S., Mural, M., Kawashima, M. Operational Experience of HSST-03 System at Expo'85 and Expo'86, International Conference on Maglev and Linear Drives, Las Vega, May 19-21, 1987.

6. Talya, I. I. USSR Inventor's Certificate No 1248176 A, "Asynchronous Tractive-Levitation System for Transport Vehicle."

7. Yepifanov, A. P., Lebedev, A. M., Talya, I. I. "Linear Asynchronous Modular-Type Drive," "Issledovaniye raboty elektrotekhnicheskikh ustroystv skorostnogo passazhirskogo transporta na magnitnoy podveske s lineynym tyagovym privodom: Sbornik nauchnykh trudey" [Study of Operation of Electrical Engineering Devices of High-Speed Passenger Transport on Magnetic Suspension With Linear Tractive Drive: Collection of Scientific Articles], Moscow, VNIIPIGidrotruboprovoda, 1988.

8. Yepifanov, A. P., Lebedev, A. M., Talya, I. I. "Increasing the Efficiency of a Tractive Linear Asynchronous Drive," IZVESTIYA VUZOV. ELEKTROMEKHANIKA, No 7, 1990.

Products of Interdepartmental Scientific-Technical Complex "ROBOT" at "Lift and Transport Technology" Exhibition

917F0319C Moscow MEKHANIZATSIYA I AVTOMATIZATSIYA PROIZVODSTVA in Russian No 4, Apr 91 pp 40-42

[Article by V.B. Velikovich, engineer, and N.Sh. Zhapparov, candidate of technical sciences]

UDC 621.86/.87

[Abstract] The interdepartmental scientific-technical complex "ROBOT", an association of over 40 enterprises in the USSR engaged in developing and building industrial robots complete with auxiliary equipment, participated in the 1990 "Lift and Transport Technology" trade exhibition. The five items which attracted the greatest interest were: 1) electric car-robot model ETR-0502 (load capacity 500 kg, full-load speed 1 m/s); 2) series of multimodular industrial robots with 10-160 kg load capacity for gantry and crane duty (electromechanical drive, position-contour control with adaptive programming, maximum positioning error +/-0.25 mm); 3) series of no-backlash planetary speed reducing gear trains (basic model featuring a transmission ratio 100:1, nominal output torque 60 N.m, maximum speed of driver 3000 rpm, maximum backlash on driven side 0.008°, efficiency 80 %); 4) hydraulic industrial shock absorbers for smooth shock-free stopping of moving objects in the kilogram-kiloton range; 5) technical vision system including solid-state linear video cameras with power supply, a microcomputer for automatic processing of visual input data and an image printer, also options such as data processing control, video display monitors operating with matrix-array cameras, and interfacing printed-circuit boards for signal transmission from video camera to microcomputer. Tables 2.

Electric Drives for Machine Tools and Robots: Status and Outlook

917F0318A Moscow VESTNIK MASHINOSTROYENIYA in Russian No 3, Mar 91 pp 33-38

[Article by G.S. Korotkov, candidate of technical sciences, A.A. Kirillov, candidate of technical sciences,

V.V. Gorchakov, candidate of technical sciences, V.M. Nikitin, candidate of technical sciences, and V.A. Nesterin, candidate of technical sciences, All-Union Scientific Research Institute of Robotics, A.I. Kondrikov, candidate of technical sciences, and M.A. Bosinzon, candidate of technical sciences, Experimental Scientific Research Institute of Metal Cutting Machine Tools]

UDC 621.9.06-83+621.865.8-83

[Abstract] The machine manufacturing industry is now undergoing a transition to technologies based on conservation of resources, quick retooling being essential if production shortfall is to be minimized. This concerns particularly automated flexible production systems, which include electrically controllable electric drives for machine tools and industrial robots. The current trends regarding motor controls are elimination of power transformers, use of multicoordinate frequency converters for speed control with encapsulated power semiconductors, and use of microprocessors with large-scale circuit integration. The most promising trend regarding drive motors is toward brushless a.c. ones: synchronous motors with permanent magnets for feed drives and two-phase squirrel-cage induction motors for transport drives. Synchronous motors available for EPB2 feed drives with transistor speed control are series DVM and DVU with 0.1-0.7/1.3-35 N.m torque ratings (maximum speeds 2000-6000/1000-4000 rpm), those available for ETS1 feed drives with thyristor speed control are series 4S2P with 47-170 N.m torque ratings (maximum speed 1500 rpm). The material of permanent magnets is either a rare-earth alloy for the DVM motors (0.01-7 N.m) or strontium ferrite for the DVU motors (7-35 N.m) and the 4S2P motors (47-170 N.m). Motors with transistor speed control for EPB2 drives are furnished with a contactless tachometer and a photopulse trajectory sensor or a position sensor, some also with an electromagnetic brake, these drives being particularly well suited for machine tools and industrial robots with numeric program control. Induction motors available for "Razmer"(Dimension) 2M-5 transport drives with transistor speed control are series 4AB2 and 4AKhB2 with 2.2-18.5 kW power ratings (maximum speeds 3000-5000 rpm), those available for ETA1-01 transport drives with thyristor speed control are series 4DCh, 4KhDCh, and 4AMMChP with 3.0-265 kW power ratings (maximum speed 2000 rpm). Thyristor speed control features direct coupling, a 3-phase/ 2-phase frequency converter being used with 4S2P synchronous motors. One significant recent development is digital motor speed control, separate from and in addition to not always adequate numeric program control of machine tools. An example is the new series of autonomous electric drives with digital control through two signal transmission channels: a standard pulsed constant-speed regulation channel and a 0.5 Mbyte fast multiplexed one. Figures 6. references 2.

Pulsed Optoelectronic Rotation Angle Transducer

917F0319A Moscow MEKHANIZATSIYA I AVTOMATIZATSIYA PROIZVODSTVA in Russian No 4, Apr 91 pp 7-10

[Article by A.N. Shilin, candidate of technical sciences, and D.V. Lyutikov, engineer]

UDC 621.374.387:531.7.08

[Abstract] A pulsed optoelectronic instrument transducer is described which measures rotation angles of tubular shells for the petrochemical industry during their fabrication. The transducer is mounted free to rotate on a carriage which can move in two orthogonal directions. It senses successive positions of one shell edge relative to the optical axis as the shell is turned around for machining. An electric d.c. lamp illuminates the shell from the other side without generating interference. The transducer output signal, pulse-width modulated, is converted into a digital code with the aid of clock pulses coming from a reference-frequency oscillator and counted in a comparator. The comparator feeds data about all points around the shell edge to a micromputer, which calculates the radius of curvature at each point and then selects the smallest one for a determination of the necessary bending radius and shell unloading cycles. Truing the shell is the next step, for which the required bending radius is preset on a sheet-metal bending machine and the shell is then turned on the rolls of that machine through a given number of revolutions. The transducer is reversible, sensing the angular position of the shell on the basis of the angle through which it has been rotated in either direction, and operates in the sequential count mode. It consists of a disk with notches uniformly spaced around its periphery and two optron pairs spaced 90° apart on its periphery, a set of electronic amplifiers, a reversing device with logic using four AND gates and two NOR gates, and a reversible electronic pulse counter with a four-position digital indicator. An experimental prototype of the information-and-measurements system including this transducer was designed, built, and tested in the laboratory at the All-Union Scientific Research, Design, and Technological Institute of Petrochemical Apparatus. It was found to operate reliably and to yield cross-sectional dimensions of a shell with a total error not larger than 1.2 mm. Figures 2.

State of the Art in Comprehensive Nondestructive Inspection Facilities

917F0286A Sverdlovsk DEFEKTOSKOPIYA in Russian No 1, Jan 91 pp 68-73

[Article by Ye.A. Gusev and F.R. Sosnin, Scientific Research Institute of Penetroscopy, Moscow]

UDC 620.179

[Abstract] The basic goal in development of multitransducer equipment for comprehensive nondestructive

inspection is facilitate recording the effects of the action of fields or particles characterizing various physical phenomena on the test object so as to cover a sufficiently wide range of effects of any one physical phenomenon within several narrow ranges of frequency and energy. No now existing apparatus satisfies all these requirements. On a 1-5 scale, three methods of inspection are by far most effective: radiographic inspection, acoustic inspection, and the eddy-current method. Their present status and development are, accordingly, of particular interest. Means now available for recording a wide range of effects of one physical phenomenon within a narrow frequency and energy range include: 1) the "American Science Engineering" model z X-ray apparatus utilizing the Compton effect for inspection of materials with high atomic numbers from z = 26 (iron) up or of materials with low atomic numbers from z = 6 (carbon) down, 2) apparatus which uses transmitted and backscattered x-rays for thickness gaging and measuring the surface density of rolled stock, 3) apparatus which uses the ultrasonic echo effect for flaw detection and inspection of welding seams in steel structures, 4) multitransducer ultrasonic apparatus for inspection of coarse-grain materials such as austenitic steels, 5) eddy-current transducers for detection of internal and surface defects. Means now available for recording the effects of one physical phenomenon within several narrow frequency and energy ranges include: 1) radiographic apparatus for inspection objects having intricate shapes and wide thickness variation, 2) multifrequency eddy-current apparatus, 3) apparatus for which combines the ultrasonic echo effect with both ultrasonic shadow and mirror-shadow effects for inspection of large aircraft components made of polymer-composite materials. Means now available for recording the effects of several phenomena on the test object include: 1) apparatus which combines x-ray Compton tomography and ultrasonic velocity measurement for inspection of such objects as raw ceramic preforms 2) "Valti" (French) system which combines ultrasonic and eddy-current inspection of tubes, 3) "Foerster" (German) system which combines an ultrasonic flaw detector and an ultrasonic thickness gage with an electromagnetic flaw detector for inspection of seamless tubes made of materials ranging from carbon-plastics to stainless steels, 4) "Sumitimo" (Japanese) system for inspection of seamless tubes which combines electromagnetic surface inspection with ultrasonic flaw detection and measurement of diameters. Many of these inspection facilities are automated with the aid of a mini- or microcomputer. With such a diversity of available inspection facilities, it is possible to select the physical phenomenon or phenomena most objectively informative about the state of the test object and to then select the most reliable inspection apparatus. Available computer technology makes, moreover, feasible not only on-line processing of complex primary data, discretization and encoding of analog signals for significance and tolerance checks, and automatic positioning of principal inspection devices, but also simple automatic regulation and self-checking. References 18.

Automation of Control and Planning of Metal Cutting Machine Tools Operation in Flexible Production Systems

917F0319B Moscow MEKHANIZATSIYA I AVTOMATIZATSIYA PROIZVODSTVA in Russian No 4, Apr 91 pp 30-33

[Article by A.A. Panov, candidate of technical sciences]

UDC 62-5:338.984

[Abstract] A control system has been designed for the metal cutting machine tools in the flexible production system at the Dnepropetrovsk Electric Locomotive Plant, an essentially decentralized control system according to the three-level scheme with microcomputers at the middle level in a radial configuration. These peripheral Elektronika-60 microcomputers drastically reduce the burden on the SM-1 main control computer at the upper level so that the response time cease to be critical, data can be stored directly at the work site without use of punched tape, and the main computer does not participate in operation of a machine tool. Decentralization also improves the reliability of the entire control system, inasmuch as failure of any one component remains localized and does not impair the rest of the system. The numeric program control for each machine tool is in this scheme directly interfaced to a peripheral microcomputer, which simplifies any necessary buildup of hardware and software without affecting the independently and uniformly operating drivers of the main computer. For operation with the upper level there are programs available which facilitate storage of the microcomputer software in the memory of the main computer and retrieval of that software back to a microcomputer before operation of its machine tool begins. For this mode of operation there are also programs available which facilitate editing the control programs and storing them on punched tape or on magnetic disks, printing them, and calling them out. For operation with the lower level there is software available which facilitates transfer of control programs from the optical reader to the microcomputer memory in a multiplex mode. The logic model for transport and storage of parts is based on a table with inventory data in rows and requisition data in columns, programs being available in the control system for changing the entries in the course of the production process. This table is checked and modified by a human operator in accordance with information from the production planning department, for each shift as well as for each week and each month. This classifies the control system as a semiautomatic one. An important role in planning and controlling the machine tool operation plays its optimization, not only with regard to machine setup and tool life but also with regard to loading schedules to meet requisitions under both technical and economic constraints. Such an optimization is a fast process, requiring only 2.5 minutes of computer time when 100 planning items are assigned to a technological unit consisting of four machine tools. The optimization algorithm is designed to select the sequence of

planning items which will minimize the amount of resetting to be done for changeover from one item to another. It is also designed to apply to any arbitrary number of machine tools in one technological unit. The metric set of all technically feasible combinations of bench, rig, and tool setup states in this control system includes the subset of all actual planning items. A noteworthy property of this set is that, whichever actual planning item has been selected as the center point of the set, all other planning items will appear as points on coaxial spheres whose radii are equal. Tables 1.

Methods of Nondestructive Flaw Detection in Dielectric Films

917F0286B Sverdlovsk DEFEKTOSKOPIYA in Russian No 1, Jan 91 pp 73-80

[Article by A.V. Gladkikh, A.A. Yevtukh, A.S. Klimenko, N.V. Moshel, and I.D. Kozhevnikova, Chernigov Pedagogical Institute imeni T.G. Shevchenko]

UDC 658.562:536.226

[Abstract] Four methods of nondestructive inspection of dielectric films are compared on the basis of their experimental evaluation on three classes of SiO_2 films: nondefective ones subject to spontaneous breakdown (SiO_2 films at an electric field intensity $E \geq 8$ MV/cm), those with surface defects, and those with through defects. Direct methods are excluded from consideration, optical microscopy on account of its limited resolution and electron microscopy on account of its complexity. The four indirect methods under consideration are: 1) use of nematic liquid crystals such as 4-methoxybenzylidene-4'-butylaniline with a negative anisotropy of the dielectric permittivity (NLC method), 2) use of copper-gelatin, 3) bubble method, 4) electric sounding. All four methods were tested on SiO_2 films, use of copper-gelatin and the bubble method by conventional techniques. The other two methods were tested on silicon structures with dielectric insulation as well as on dielectric insulation of n-S and p-Si. Use of nematic liquid crystals was tested in a NLC-SiO_2-Si configuration in polarized light for sensitivity, geometrical resolution, and reproducibility of results. Having been found to be the most informative of these methods, it was also tested for the dependence of the number of defects it reveals on the length of inspection time, on the composition of the liquid-crystal mixture, on the thickness of the liquid-crystal layer, and on the heat treatment of the holding fixture. These factors were found not to influence the reproducibility of inspection results obtained and uncontrollable impurities in a nematic liquid crystal as well as products of electrochemical reactions including ionic ones, essentially organic substances, accumulating in the course of repetitive inspection cycles were, moreover, found to evaporate even under atmospheric pressure. For repetitive inspection, nevertheless, they need to be periodically washed away from the inspection site. This method can serve as the reference standard for certification of other methods of inspecting dielectric films for continuity, while the the less sensitive but simpler bubble method is recommended for operational product quality control after it has been thus certified. Figures 3; tables 3; references 9.

Dosimeter for Industrial Betatrons

917F0286C Sverdlovsk DEFEKTOSKOPIYA in Russian No 1, Jan 91 pp 93-95

[Article by V.G. Volkov and M.M. Shteyn, Scientific Research Institute of Penetroscopy, Tomsk]

UDC 621.386.82(088.8)

[Abstract] A precision dosimeter with temperature stabilization for monitoring bremsstrahlung has been developed for MIB-4, MIB-6, and B-18 industrial betatrons now manufactured on a small scale. The dosimeter consists of a detector with a preamplifier followed by a signal processor. The detector is a feed-through ionization chamber with plane-parallel electrodes which does not produce a shadow image on x-ray film, placed in front of the radiation source and supplied from a 200 V voltage source. Its overall size is 25x100x120 mm^3, sensing action being effective within a 100 cm^3 large volume. Inside the chamber are installed a filter of electrons, its thickness depending on the maximum energy of accelerated electrons (2, 3, 9 g/cm^2 in MIB-4, MIB-6, B-18 betatrons respectively), a thermistor, and an impedance load across which a 2-3 V output signal will appear. The chamber is not hermetic so that a change in the ambient atmospheric pressure gives rise to an additional measurement error. The signal processing module contains an amplifier on a 140UD14 integrated-circuit chip with negative feedback and two outputs, the thermistor across one of them minimizing the measurement error due to temperature changes. The radiation dose is measured with an instrument which includes a voltage-to-frequency converter, a pulse counter, a programmable switch, a digital comparator, a decoder, an actuator, and an array of indicator lights (light-emitting diodes). The dose intensity is measured with an instrument which includes sensitivity regulation by means of an adjustable resistor. With a sensitivity of 0.1 R/reading, this dosimeter can measure radiation doses of up to 99.9 R. It was tested with MBI-4 and MBI-6 betatrons, being exposed to radiation fields of 0.01-100 R/min intensity. The measurement error did not exceed 3 %, temperature changes from 10°C up to 50°C causing an additional error of 0.4 % per 10°C temperature rise. The dosimeter is suitable for monitoring both radiation dose and dose power in sources of 4-25 MeV bremsstrahlung. Figures 1; references 3.

Stabilization and Extremal Properties of Bipedal Resonance

917F0324A Moscow PRIKLADNAYA MATEMATIKA I MEKHANIKA in Russian No 2, 1991 pp 193-200

[Abstract of article by V. V. Beletskiy and M. D. Golubitskaya]

UDC 531.36 : 62—50

[Abstract] A simple model of anthropomorphic bipedal motion was constructed to validate the supposition that the functional of the energy spent to walk bipedally achieves a minimum when the motion is well organized, stable, and periodic. The model was based on the motion of a bipedal walking apparatus consisting of a body and two weightless single-jointed legs joined to the body at a single point by an articulated joint. It was assumed that the motion of the apparatus is supported at a single point and takes place without impact and that the constraint is one-sided. The basic motion studied was a periodic motion during which the body of the apparatus oscillated once for each step taken by the apparatus. A law was formulated to stabilize the motion of the body during comfortable walking, thus making it possible to generate a family of non-periodic gaits close to the basic motion studied. The energy spent on the periodic and non-periodic gaits was compared, and a localized minimum for the energy-expenditure functional was established for stable resonant bipedalism. Figures 8; reference 13: Russian.

Synopses From 'Construction Materials'

917F0341A Moscow STROITELNYYE MATERIALY in Russian No 5, 1991 p 31

Abstracts of articles appearing in "Construction Materials", No 5, 1991]

[Text]

UDC 678.05.004.69

Promising Technologies and Forms of Organizing Repair Work at Enterprises of Roofing Industry Under Conditions of Economic Reform. Teplova, L. A., pp 6-9.

The experience of using leading technologies and forms of organizing repair of manufacturing equipment in production of roofing and waterproofing materials is generalized. Promising methods of volumetric and surface strengthening and also of restoration of worn parts of machines using traditional and nontraditional heat sources are considered. The characteristics of organizing a lease contract and a collective contract in the repair industry of enterprises under conditions of economic reform were determined. Introduction of leading technologies and forms of organizing repair work is an important reserve for increasing the efficiency of main production at enterprises that manufacture roofing and waterproofing materials. 8 References.

UDC 661.321.002.68:691

Porous Concrete Products Based on Lime-Containing Binder From Solid Wastes of Soda Industry. Shatov, A. A., pp 9-10.

The possibility of using solid wastes of the soda industry as a basic raw material, after corresponding heat treatment, for production of small blocks of cellular concrete, the main technical-economic indicators and the characteristics are considered. Practical application of the indicated blocks in construction is shown.

UDC 622.271.4.004.8

Ekibastuz Basin in Production of Construction Materials. Kalmykova, L. F., Kapustin, A. P., Bulyga, L. L., p 11.

Problems of integrated use of overburden rock of coal mining in production of ceramic products of a wide nomenclature and of porous fillers, burnt rock of coal mining and ashes in production of concrete are considered. Data are presented on the physicochemical and technological properties of coal wastes. The results of pilot plant tests, of introduction of developed production processes at enterprises of the construction industry of the Pavlodar-Ekibastuz territorial production complex are outlined.

UDC 691:693(-202)

Farm Outbuildings of Farmstead, and Construction Materials for Them. Volkov, A. M., Muravyev, Yu. A., pp 14-17

Economical outbuildings of a farmstead and more feasible variants of using construction materials for erection of them are considered. Three types of economical outbuildings are proposed as a function of the set of special buildings. Methods of erecting the structures are shown. 3 Figures.

UDC 678.01.001

Composite Finishing Materials of Wood Fibers and Thermoplasts. Shapovalov, V. M., Barsukov, V. G., Lapshina, Ye. N., Gubkin, V. I., pp 18-20.

The possibility of producing distillate and tile finishing composites based on wood fibers and thermoplasts was considered. The characteristics and conditions of joining wood fibers and thermoplasts, and also the role of a fiber filler in the composite were studied. It is shown that the reinforcing effect of wood fibers is manifested to the greatest extent when filling the composites—45-57% (by mass). It is established that introduction of secondary thermoplasts in the amount of 5-15% to the composite, along with improving its processing contributes to formation of high operating properties of the material. The proposed composite materials permit one to expand the variety of finishing elements, industrial and civil construction. 2 Figures, 2 tables, 4 references.

UDC 69.024.15.002

New Fused-on Roofing Material Rubelastobite of Increased Flexibility and Crack Resistance. Ivanov, V. V., Bashmachenkova, V. N., pp 20-22.

The results of modifying the mastic for roofing materials are presented. The main design principles of the composition of the mastic for roofing materials are considered, which permit one to establish optimum relations between the thermoplast and elastomer in the asphalt-polymer composite. The highly elastic mastic elastobite is proposed. It is shown that a new highly elastic fused-on roofing material of increased flexibility and crack resistance can be produced by directional modification of the structure of the mastic for roofing materials. A combination of the most favorable indicators of the construction and operating properties corresponds to these indicators, which is of considerable importance for increasing the longevity of combination roofing material of the fused-on type. 1 Table, 8 references.

UDC 666.964.658.562

Quality Control of Glue Compounds in Breathing Roofs. Ustinov, B. S., pp 23-25.

Concepts on the status of quality control of construction materials, specifically of roofing compounds, and of its significance in practical application of the latter are advanced. A device is proposed for testing roofing compounds, which permits one to determine the operating qualities of the materials for soft roofs and to predict their reliability on the basis of experimental studies. The device is described and its operating principle is discussed.

UDC 666.946.2.622.692.47

Using Gas-Filled Systems in Construction of Oil and Gas Wells and in Housing Construction. Dulayev, V. Kh.-M., Petresku, V. I., Polukhina, N. A., Chernykh, V. F., pp 26-27.

The possibility of using gas-filled plugging systems in construction of oil and gas wells is considered. Effective methods of introducing the gas phase to a gas-filled deposit are shown. Chemical gas producers, which permit one to obtain stable gas-generating systems, are proposed. Their physicochemical characteristics are presented. Gas-filled systems can be used in production of construction materials for house building, specifically, in manufacture of cellular concretes. 1 Figure.

NTIS
ATTN PROCESS 103
5285 PORT ROYAL RD
SPRINGFIELD VA 22161

2

Foreign Broadcast Information Service (FBIS) and Joint Publications Research Service (JPRS) publications contain political, military, economic, environmental, and sociological news, commentary, and other information, as well as scientific and technical data and reports. All information has been obtained from foreign radio and television broadcasts, news agency transmissions, newspapers, books, and periodicals. Items generally are processed from the first or best available sources. It should not be inferred that they have been disseminated only in the medium, in the language, or to the area indicated. Items from foreign language sources are translated; those from English-language sources are transcribed. Except for excluding certain diacritics, FBIS renders personal and place-names in accordance with the romanization systems approved for U.S. Government publications by the U.S. Board of Geographic Names.

Headlines, editorial reports, and material enclosed in brackets [ ] are supplied by FBIS/JPRS. Processing indicators such as [Text] or [Excerpts] in the first line of each item indicate how the information was processed from the original. Unfamiliar names rendered phonetically are enclosed in parentheses. Words or names preceded by a question mark and enclosed in parentheses were not clear from the original source but have been supplied as appropriate to the context. Other unattributed parenthetical notes within the body of an item originate with the source. Times within items are as given by the source. Passages in boldface or italics are as published.

SUBSCRIPTION/PROCUREMENT INFORMATION

The FBIS DAILY REPORT contains current news and information and is published Monday through Friday in eight volumes: China, East Europe, Soviet Union, East Asia, Near East & South Asia, Sub-Saharan Africa, Latin America, and West Europe. Supplements to the DAILY REPORTs may also be available periodically and will be distributed to regular DAILY REPORT subscribers. JPRS publications, which include approximately 50 regional, worldwide, and topical reports, generally contain less time-sensitive information and are published periodically.

Current DAILY REPORTs and JPRS publications are listed in *Government Reports Announcements* issued semimonthly by the National Technical Information Service (NTIS), 5285 Port Royal Road, Springfield, Virginia 22161 and the *Monthly Catalog of U.S. Government Publications* issued by the Superintendent of Documents, U.S. Government Printing Office, Washington, D.C. 20402.

The public may subscribe to either hardcover or microfiche versions of the DAILY REPORTs and JPRS publications through NTIS at the above address or by calling (703) 487-4630. Subscription rates will be provided by NTIS upon request. Subscriptions are available outside the United States from NTIS or appointed foreign dealers. New subscribers should expect a 30-day delay in receipt of the first issue.

U.S. Government offices may obtain subscriptions to the DAILY REPORTs or JPRS publications (hardcover or microfiche) at no charge through their sponsoring organizations. For additional information or assistance, call FBIS, (202) 338-6735,or write to P.O. Box 2604, Washington, D.C. 20013. Department of Defense consumers are required to submit requests through appropriate command validation channels to DIA, RTS-2C, Washington, D.C. 20301. (Telephone: (202) 373-3771, Autovon: 243-3771.)

Back issues or single copies of the DAILY REPORTs and JPRS publications are not available. Both the DAILY REPORTs and the JPRS publications are on file for public reference at the Library of Congress and at many Federal Depository Libraries. Reference copies may also be seen at many public and university libraries throughout the United States.